

Gamma-ray Line Astronomy *

R. Diehl^a †

^aMax-Planck-Institut für extraterrestrische Physik, D-85741 Garching, Germany

Gamma-ray lines from radioactive isotopes, ejected into interstellar space by cosmic nucleosynthesis events, are observed with new space telescopes. The Compton Observatory had provided a sky survey for the isotopes ^{56}Co , ^{22}Na , ^{44}Ti , and ^{26}Al , detecting supernova radioactivity and the diffuse glow of long-lived radioactivity from massive stars in the Galaxy. High-resolution spectroscopy is now being exploited with Ge detectors: Since 2002, with ESA's INTEGRAL satellite and the RHESSI solar imager two space-based Ge-gamma-ray telescopes are in operation, measuring Doppler broadenings and line shape details of cosmic gamma-ray lines. First year's results include a detection and line shape measurement of annihilation emission, and ^{26}Al emission from the inner Galaxy and from the Cygnus region. ^{60}Fe gamma-ray intensity is surprisingly low; it may have been detected by RHESSI at 10% of the ^{26}Al brightness, yet is not seen by INTEGRAL. ^{44}Ti emission from Cas A and SN1987A is being studied; no other candidate young supernova remnants have been found through ^{44}Ti . ^{22}Na from novae still is not seen.

1. INTRODUCTION

Radioactive isotopes as common by-products of nucleosynthesis in cosmic sources can be studied through their gamma-ray emission [5]. Candidate sources are supernovae and novae, but also the winds from massive stars. Continuum emission from Comptonized or thermalized radioactive energy is also exploited as a measurement of nucleosynthesis, but less direct: Conversion of original radioactive energy must be calculated through complex radiation transport models. Alternatively, characteristic isotopic samples of the nucleosynthesis source, as conserved in circum-source dust grains, allow significant nucleosynthesis inferences, in particular on AGB stars, but more recently even on supernovae and novae. But here the physics of dust condensation near the production site, and transport and processing history of such grains is uncertain. Other measurements of cosmic nucleosynthesis are also rather indirect, e.g. the analysis of X-ray line emission from ionized-gas portions of supernova remnants and galactic-halo gas. Radioactive decay in interstellar space is unaffected by physical conditions in/around the source such as temperature or

*accepted for *Nucl.Phys.A (Proc. NIC8, Vancouver 2004)*

†INTEGRAL/SPI results reported here have been obtained through collaborative efforts of the team of SPI scientists, thanks to the excellent performance which resulted from the dedication of SPI detector and subsystem experts, ESA mission operations and the Russian launch vehicle. SPI has been completed under the responsibility and leadership of CNES. We are grateful to ASI, CEA, CNES, DLR, ESA, INTA, NASA and OSTC for support.

density, and decay gamma-rays are not attenuated along the line-of-sight due to their penetrating nature (attenuation length \simeq few g cm^{-2}). Therefore, such decay gamma-rays with satellite-borne telescopes provide the most direct measurement of the existence of freshly-produced isotopes.

Various gamma-ray telescope experiments have established this new window for the study of cosmic nucleosynthesis during the past three decades [5]:

- Interstellar ^{26}Al has been mapped along the plane of the Galaxy, confirming that nucleosynthesis is an ongoing process [6, 37, 35].
- Characteristic Ni decay gamma-rays have been observed from SN1987A [48, 30, 23], directly confirming supernova production of fresh isotopes up to iron group nuclei.
- ^{44}Ti gamma-rays have been discovered [11, 42] from the young supernova remnant Cas A, confirming models of α -rich freeze-out for core-collapse supernovae.
- A diffuse glow of positron annihilation gamma-rays has been recognized from the direction of the inner Galaxy [38, 15], consistent with nucleosynthetic production of β^+ -decaying radioactive isotopes

These results have led to new questions:

- What fraction of radioactive energy is converted into other forms of energy in supernovae? (This addresses: absolute normalization of indirectly-inferred radioactive amounts from ^{56}Ni in SNIa, and ^{44}Ti in core-collapse SNe; positron leakage from supernovae; morphology of expanding supernova envelopes, "bullets", filaments, jets).
- How good are our (basically one-dimensional) models for nova and supernova nucleosynthesis, in view of important 3D effects such as rotation and convective mixing? (This addresses: ^{44}Ti mass ejected from regions near the mass cut between compact remnant and ejected supernova envelope; nova ^{22}Na yields and the seed compositions for explosive hydrogen burning in novae).
- What is the range of physical conditions expected for nucleosynthesis events? (This addresses: stellar mass distributions and supernova rates in massive-star clusters; clustering of events in space and time; self-enrichment; triggered star formation in dense, active nucleosynthesis regions; first stellar generations when metallicity was extremely low).
- How are ejecta and energy from nucleosynthesis events fed back into the interstellar medium? (This addresses: scales and time constants of chemical evolution of interstellar gas; morphology of the interstellar medium; spatial pattern of star formation; nucleation of dust and its processing by interstellar shocks; acceleration of cosmic rays)

With INTEGRAL and RHESSI, now a new step is taken, improving sensitivities by \simeq an order of magnitude: The spectrometer SPI [49, 41] on INTEGRAL [52] is based on 19 hexagonal Ge detector modules, each one 7 cm thick and 5.5 cm wide (flat-to-flat

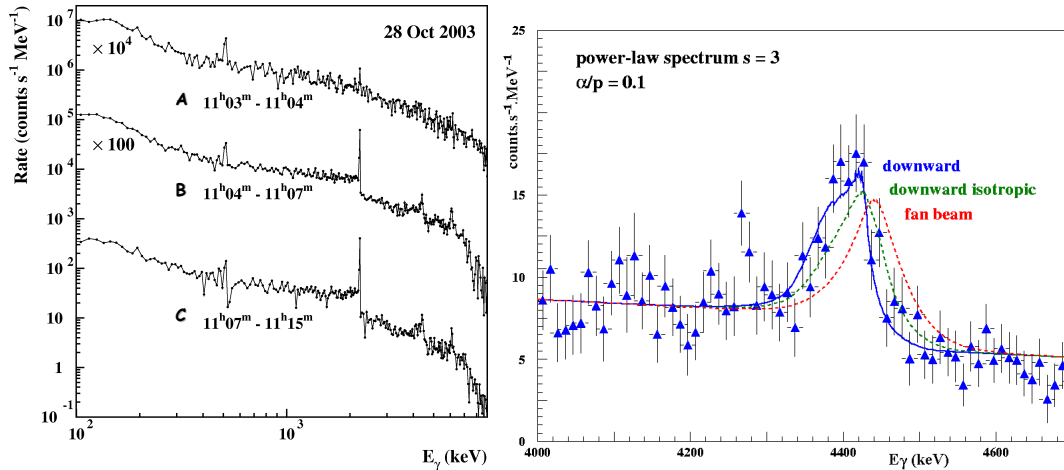


Figure 1. SPI measurement of the spectral variations over three successive phases of the Oct 28 solar flare (left). The ^{12}C line shape from late flare phases (B,C) is compared with models for different geometries of the accelerated particle beam (right) (see [7]).

across their hexagonal shape), arranged in a densely packed detector plane of 500 cm² total area. Failure of two of the detector modules (#2 in Dec 2003, #17 in July 2004) has reduced the effective area now by $\simeq 10\%$. The Ge detectors are illuminated through a coded mask made of 3 cm of tungsten, defining a telescope field-of-view of 16°. Detector temperature is maintained at $\simeq 90$ K by Stirling coolers. The accumulated damage from cosmic-ray bombardment in the detector crystals leads to $\simeq 10\%$ degradation of spectral resolution and an asymmetric response. This is cured every $\simeq 6$ months by heating up the camera to $\simeq 105^\circ\text{C}$ for $\simeq 1.5$ days ("annealing"), a procedure which has been exercised successfully in orbit four times already, re-establishing the original spectral response and resolution of $\simeq 3$ keV at 2 MeV. Complementing this, the RHESSI solar observatory satellite [26] with its imaging spectrometer instrument carries similar fine-spectroscopy Ge crystals. Although pointed at the Sun, this has proven sensitive enough for diffuse cosmic gamma-ray emission studies, when using the Earth as a shadowing device. With these instruments, we now can observe kinematic signatures from Doppler-shifted energy values in expanding/accelerated radioactive material from sources of cosmic nucleosynthesis.

2. RESULTS

In their first two mission years, INTEGRAL and RHESSI results have already demonstrated the useful complement of such measurements for the field:

- Solar flare observations allowed measurements of flare spectra and in particular excited-particle flow geometries [27, 43, 7].
- Gamma-ray line emission from ^{26}Al and positron annihilation have been measured, imaging their sources in the Galaxy, and determination of source velocity characteristics is underway [4, 17, 13, 9].

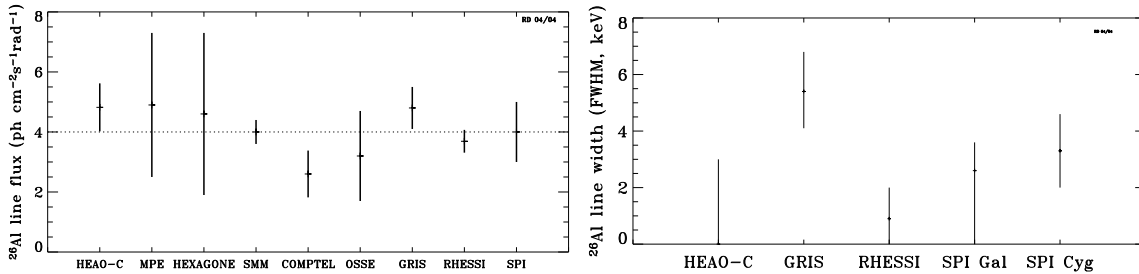


Figure 2. Intensity measurements (left) and line width measurements (right) from different experiments for ^{26}Al emission from the inner Galaxy, and for Cygnus (rightmost datapoint).

- Search for ^{60}Fe emission has been partly successful, with a marginal RHESSI result and new limits from INTEGRAL [44, 43, 16].
- Search for ^{44}Ti emission from Cas A and SN1987A, and from unknown but expected sources in the inner Galaxy is underway [40, 50].

2.1. Solar Flares

Gamma-ray spectroscopy of solar flares is a prime diagnostic of particle acceleration mechanisms, the Sun a unique nearby laboratory. Ions are energized in the solar magnetosphere and collide with matter of the upper solar atmosphere. Collisionally-excited nuclei de-excite, emitting characteristic gamma-ray lines. The physical process and energy source of particle acceleration are essentially unknown; their study is the main objective of the RHESSI space experiment. Imaging the footpoints of gamma-ray emission with respect to the flare loops, interesting offsets for neutron capture versus de-excitation lines have been revealed [27, 43]. For one of the stronger recent flares, also INTEGRAL's spectrometer measured C and O line shapes, even improving on RHESSI's spectroscopic precision. Observed line redshifts are rather well determined and consistent with downward beaming of energetic particles. Here, the beam geometry could be constrained to a narrow downward-directed one, rather than isotropic or fan-like [7] (see Fig.1).

2.2. Interstellar ^{26}Al and ^{60}Fe

Precision follow-up measurements of 1808.7 keV emission from Galactic ^{26}Al have been one of the main science goals of the INTEGRAL mission [52], after the COMPTEL sky survey [35, 21, 34, 6] had mapped structured ^{26}Al emission, extended along the plane of the Galaxy. Models of ^{26}Al emission from the Galaxy and specific localized source regions have been based on knowledge about the massive-star populations, and suggest that such stars dominate ^{26}Al production in the Galaxy [37, 19, 20]. Galactic rotation and dynamics of the ^{26}Al gas ejected into the interstellar medium are expected to leave characteristic imprints on the ^{26}Al line shape [22]. In particular after the GRIS balloon experiment reported a significantly-broadened line [33], which translates into a Doppler broadening of 540 km s $^{-1}$, alternative measurements of the ^{26}Al line shape have been of great interest. Considering the 1.04×10^6 y decay time of ^{26}Al such a large line width is

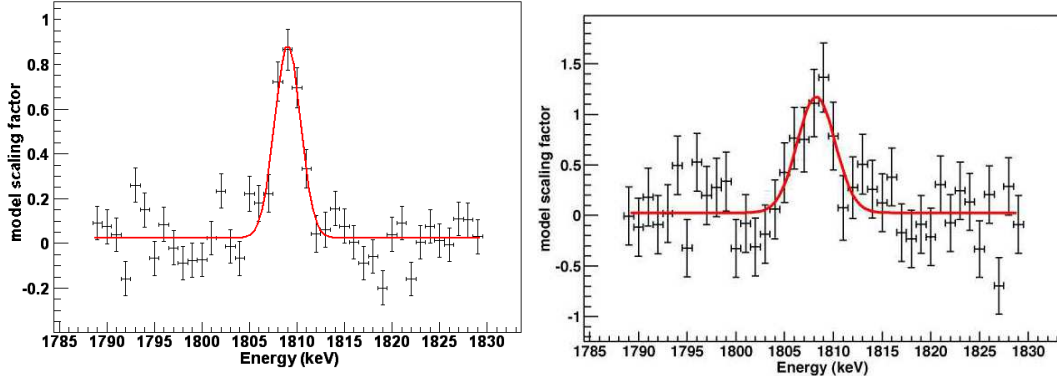


Figure 3. SPI ^{26}Al line spectra for the inner Galaxy (left) and the Cygnus region (right). The spectra are derived by fitting skymap intensities per energy bin. Exposures are $\simeq 4\text{Msec}$ each, from the Core Program inner-Galaxy survey, and from Cygnus region calibrations and Open-Program data.

hard to understand, and requires either kpc-sized cavities around ^{26}Al sources or major ^{26}Al condensations on grains [2, 46].

Current results on large-scale Galactic ^{26}Al line flux and width measurements are summarized in Fig. 2. From INTEGRAL/SPI spectral analysis of a subset of the first-year’s inner-Galaxy deep exposure (“GCDE”), ^{26}Al emission was clearly detected (Fig. 3 left) [4, 3] ($5\text{--}7\sigma$; through fitting of adopted models for the ^{26}Al skymap to all SPI event types over an $\simeq 80\text{ keV}$ energy range around the ^{26}Al line). The line width was found consistent with SPI’s instrumental resolution of 3 keV (FWHM). Therefore, these early SPI results support RHESSI’s recent finding [44] that the broad line reported by GRIS [33] probably cannot be confirmed (Fig. 2). On the other hand, the first spectrum generated from SPI data for the Cygnus region (see Fig. 3 right for single-detector events [17]) suggests that the line may be modestly broadened for this region. This may be caused by locally-increased interstellar turbulence in the particularly young stellar associations of Cygnus.

The fact that ^{60}Fe has not been clearly seen from the same source regions appears surprising [36], given that ^{26}Al -ejecting massive stars are expected to also eject ^{60}Fe in substantial amounts [47, 25]. RHESSI reported a marginal signal [43] at the 10%-level of ^{26}Al brightness, and also SPI’s upper limit is substantially below the ^{26}Al brightness [16]. If massive stars are the dominating ^{26}Al sources, recent models of nucleosynthesis (see [36, 25]) even increase ^{60}Fe production in late evolutionary phases near the supernova at the bottom of the He shell, or even more efficiently in the C shell. This is mainly due to increased neutron capture cross sections for Fe isotopes, and a reduced ^{59}Fe β -decay rate. The now-expected ratio falls in a range between 40 and 120%, depending on how the interpolation between the few calculated stellar-mass gridpoints is done, and which of the models are taken as baseline; in comparison, the IMF choice appears uncritical. In any case, revised expectations clearly lie above the experimental limits for Galactic ^{60}Fe emission (Fig. 4); the answer may be found in model detail, possibly in nuclear-physics

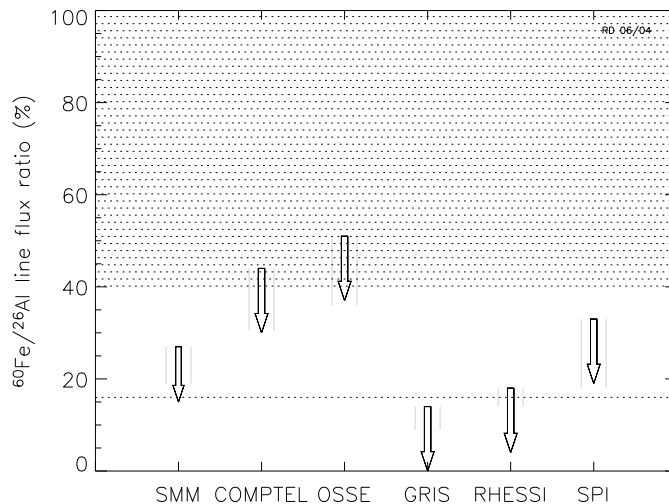


Figure 4. Limits on the ^{60}Fe to ^{26}Al gamma-ray brightness ratio, from several experiments fall below current expectations: An often-cited theoretical value from the Santa Cruz group [47] is indicated as dotted line, the dotted area marks the regime suggested by recently-updated models, from [36].

issues related to the (uncertain) Fe neutron capture reactions.

2.3. Positron Annihilation

Positrons (e^+) are produced upon β^+ -decay of proton-rich unstable isotopes. Other sources are expected to contribute to the e^+ budget, however: Plasma jets ejected from pulsars [53, 14] or microquasars [32] will produce e^-e^+ beams as a consequence of rotational magnetosphere discharges or accretion, respectively, and annihilation of dark-matter particles attracted by the gravitational potential of the Galaxy may produce distributed e^-e^+ pairs [1]. The fractional contribution from nucleosynthesis sources to the e^+ budget within the inner Galaxy regions is estimated to range from $\simeq 30\%$ to 100% (mainly SNIa and novae through ^{56}Co , ^{13}N , and ^{18}F). Substantial uncertainty in e^+ yields arises from the unknown e^+ escape fractions from these sources. A lower limit is placed from observed ^{26}Al , at $\simeq 3 \cdot 10^{-4} \text{ ph cm}^{-2}\text{s}^{-1}$.

The intensity in the annihilation line is $9.9_{-2.2}^{+4.7} \times 10^{-4} \text{ ph cm}^{-2}\text{s}^{-1}$, as derived from first analysis of SPI data from a part of the inner-Galaxy deep exposure (GCDE) of the first mission year [29, 13] (see Fig.5), which is consistent with previous measurements and theoretical predictions. This corresponds to a positron production rate in the inner Galaxy on the order of 10^{43}s^{-1} for an assumed steady state [39].

Positrons with high energies have a low probability for annihilation. Generated at typical energies of $\simeq \text{MeV}$, only a small fraction will annihilate before thermalization along their trajectories in the ISM. Once thermalized, positrons annihilate preferentially through the intermediate formation of positronium atoms, or on the surface of charged dust particles. This leads to different gamma-ray spectral components from each of these annihilation channels, a composite shape of the 511 keV line and an underlying Ps continuum

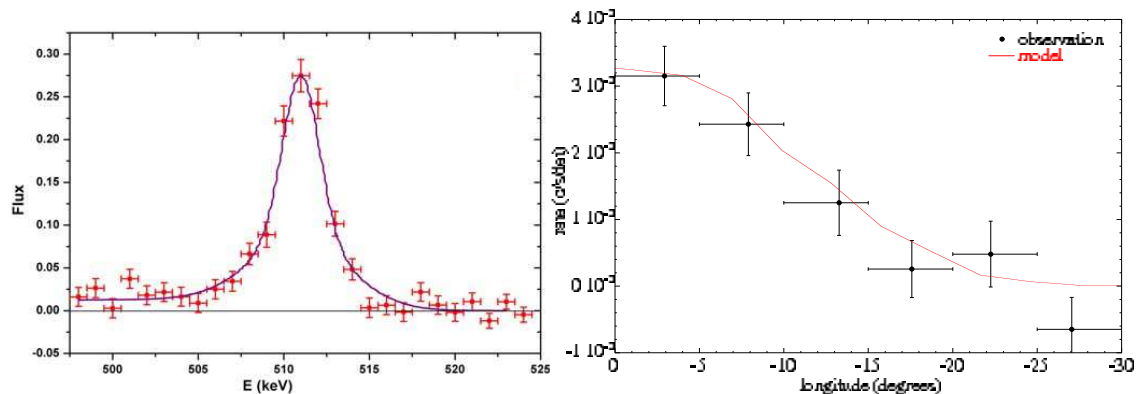


Figure 5. SPI measurement of the positron annihilation gamma-ray line from the inner Galaxy. The line is confirmed to be intrinsically broadened [29] (left: intensity in units $10^{-4}\text{ph cm}^{-2}\text{s}^{-1}$ for 1 keV wide bins, fitted with a composite model of gas and dust, from [9]). The positron annihilation gamma-ray line intensity in the inner Galaxy as observed with SPI, compared to the longitude distribution expected from a Gaussian-distributed model [13] (right).

[8]. Detailed 511 keV line shape measurements are an important diagnostic, (a) because its measurement is easier with high spectral-resolution experiments than constraining the spectrally-distributed and background-contaminated continuum, and (b) because the details of the annihilation line shape will encode kinematics and thermal properties of the annihilation regions. As a complication, the lifetime of \simeq MeV positrons in interstellar space can be substantial [8], up to 10^5 y, so that positrons may travel significant (few 100 pc) distances between their sources and the locations of their annihilation.

SPI detects Ps continuum [45] and 511 keV line [13], and finds the line to be significantly broadened, from deconvolution with the instrumental resolution after subtraction of the (strong) instrumental background line [29]. The SPI value of $2.95(\pm 0.6)$ keV (FWHM) is on the high side of values measured by previous instruments (HEAO-C [28]: 1.6 ± 1.3 ; GRIS [24]: 2.5 ± 0.4 ; TGRS [10]: 1.81 ± 0.54). First composite source process models suggest that annihilation on grains are a significant contribution, in order to obtain a sufficiently narrow line profile satisfying the SPI measurement [9].

A diffuse nature of the source is expected both from radioactive and from dark matter sources, while localized emission / hot spots would be expected if annihilation near compact sources (microquasars, pulsars) is significant. Therefore, models to interpret previous measurements with instruments of rather modest (few degrees) imaging resolution have been composed from disk contributions (diffuse radioactivity from bulge and disk novae and other sources, or latitudinally more-extended warm or hot ISM gas models) and from point sources for candidate e^-e^+ producers such as 1E 1740.7-2942.

From OSSE scans of the inner Galaxy with its field-of-view of $11.4 \times 3.8^\circ$, the spatial distribution was found to be best represented by a Gaussian with an extent of $\simeq 5^\circ$ (FWHM) in longitude and latitude [15, 31]. Surprisingly, only a minor disk-like component was observed, and the "bulge" component appeared rather extended; furthermore, there was

indication of asymmetry [38], with an excess of annihilation emission in the northern hemisphere towards latitudes of $\simeq 10^\circ$. Yet, no mapping of annihilation emission was available along the disk of the Galaxy outside this inner region; this is one of the current projects for the SPI instrument on INTEGRAL.

SPI data [13, 18] confirm OSSE's findings: The 511 keV line flux, as it varies for different exposures successively pointed along the plane of the Galaxy (Fig. 5) suggests that diffuse emission extends over a large volume. A Gaussian spatial distribution is constrained to an extent (FWHM) of 6° – 18° [13, 51]. First imaging attempts do not show signs of asymmetry, but confirm the extended and rather smoothly-distributed emission, both in longitude and latitude [18]. There is no hint for emission from the disk of the Galaxy yet; such emission must exist at some level, however, due to the positrons emitted by nucleosynthesis sources in the disk. The image also suggests that annihilation near localized sources (in particular microquasars, pulsars, or individually-bright supernovae) does not dominate the e^+ budget in the inner Galaxy, and rather a large number of sources distributed over a larger region, or distributed source processes, provide the origin of positrons.

3. Summary and Outlook

Measurement of characteristic gamma-rays from radioactive isotopes provides a useful complement to other means of the study of cosmic nucleosynthesis. Ge spectrometers have been deployed in space, capable to measure details of characteristic gamma-ray lines with sufficient precision to directly constrain abundances and kinematics of freshly-produced radio-isotopes and positrons. The diffuse ^{26}Al line has been found to be rather narrow. 511 keV emission appears dominated by an extended source region in the inner Galaxy; dust plays a significant role in the annihilation process. Neither new ^{44}Ti [40] nor ^{22}Na [12] sources have been found; analysis for ^{44}Ti from Cas A and SN1987A is in progress. INTEGRAL is scheduled to observe the gamma-ray sky for at least six years, promising to significantly advance our understanding of supernovae and novae, and of the interstellar medium embedding the sources of nucleosynthesis.

REFERENCES

1. Boehm C., Hopper D., Silk J., *et al.*, *Phys.Rev.Lett* **92**, 1301 (2004).
2. Chen W., Diehl R., Gehrels N., *et al.*, *ESA-SP*, **382**, 105 (1997).
3. Diehl R., Kretschmer K., Lichti G.G., *et al.*, *ESA-SP*, **552**, *in press* (2004).
4. Diehl R., Knödlseeder J., Lichti G.G., *et al.*, *A&A*, **411**, L451 (2003).
5. Diehl R., and Timmes F.X., *PASP*, **110**, **748**, 637 (1998).
6. Diehl R., Dupraz C., Bennett K., *et al.*, *A&A*, **298**, 445 (1995).
7. Gros M., Tatischeff V., Diehl R. , *et al.*, *ESA-SP*, **552**, *in press* (2004).
8. Guessoum N., Ramaty R., Lingenfelter R.E. , *ApJ*, **378**, 170 (1991).
9. Guessoum N., Jean P., Knödlseeder J. , *et al.*, *ESA-SP*, **552**, *in press* (2004).
10. Harris M.J., Teegarden B.J., Cline T.L., *et al.* , *ApJ*, **501**, L55 (1998).
11. Iyudin A. F., Diehl R., Bloemen H., *et al.*, *A&A*,**284**, L1 (1994).
12. Jean P., Knödlseeder J., Hernanz M. *et al.*, *ESA-SP*, **552**, *in press* (2004).
13. Jean P., Vedrenne G., Roques J.-P., *et al.*, *A&A*, **407**, L55 (2003).

14. Kennel C.F., and Coroniti F.V., *ApJ*, **283**, 694 (1984).
15. Kinzer R. *et al.*, *ApJ*, **559**, 705 (1999).
16. Knödlseeder J., Cisana E., Diehl R. *et al.*, *ESA-SP*, **552**, *in press* (2004a).
17. Knödlseeder J., Valsesia M., Allain M. *et al.*, *ESA-SP*, **552**, *in press* (2004b).
18. Knödlseeder J., Lonjou V., Jean P., *et al.*, *A&A*, **411**, L457 (2003).
19. Knödlseeder J., Bennett K., Bloemen H., *et al.*, *A&A*, **344**, 68 (1999).
20. Knödlseeder J. , *ApJ*, **510**, 915 (1999).
21. Knödlseeder J., Dixon D., Bennett K., *et al.* , *A&A*, **345**, 813 (1999).
22. Kretschmer K., Diehl R., Hartmann D.H., *A&A*, **412**, 47 (2003).
23. Kurfess J. D., Johnson W. N., Kinzer R. L., *et al.*, *ApJL*, **399**, L137 (1992).
24. Leventhal M., Barthelmy S.D., Gehrels N., *et al.*, *ApJ*, **405**, L25 (1993).
25. Limongi M. , *this conference*
26. Lin R.P., Dennis B.R., Hurford G.J., *et al.*, *Sol.Phys.*, **210**, 3 (2002).
27. Lin R.P., Dennis B.R., Hurford G.J., *et al.* , *ApJL*, **595**, L69 (2003).
28. Mahoney W. A., Ling J.C., Wheaton W.A., Lingenfelter R.E. , *ApJS*, **92**, 387 (1994)
29. Lonjou V., Weidenspointner G., Knödlseeder J., *et al.*, *ESA-SP*, **552**, *in press* (2004).
30. Matz S., Share G.J., Leising M.D., *et al.*, *Nat.*, **331**, 416, (1988).
31. Milne P., Kurfess J., Kinzer R.E., *et al.*, *AIP Conf. Proc.*, **587**, 11 (2001).
32. Mirabel I.F., Rodriguez L.F., Cordier B., *et al.*, *Nat.*, **358**, 215 (1992).
33. Naya J. E., Barthelmy S.D., Bartlett L.M., *et al.*, *Nat*, **384**, 44 (1996).
34. Oberlack, U., *Ph. D. Thesis, Technische Universität München* (1997).
35. Plüschke, S., Diehl, R., Schönfelder, V., *et al.*, *ESA SP*, **459**, 55 (2001).
36. Prantzos, N., *A&A*, **420**, 1033, (2004).
37. Prantzos, N., and Diehl, R., *Phys. Rep.*, **267**, 1, (1996).
38. Purcell W.R., Cheng L.-X., Dixon D.D., *et al.*, *ApJ*, **491**, 725 (1997).
39. Ramaty R., Skibo J., Lingenfelter R.E., *ApJS*, **92**, 393 (1994).
40. Renaud M., Lebrun F., Ballet J., *et al.*, *ESA-SP*, **552**, *in press* (2004).
41. Roques J.-P., Schanne S., von Kienlin A., *et al.*, *A&A*, **411**, L91 (2003).
42. Schönfelder V., Bloemen H., Collmar W., *et al.*, *AIP Conf Proc*, **510**, 54 (2000).
43. Smith D., *ESA-SP*, **552**, *in press* (2004).
44. Smith, D. , *ApJ*, **589**, L55 (2003).
45. Strong A.W., Diehl R., Halloin H., *et al.*, *ESA-SP*, **552**, *in press* (2004).
46. Sturmer S. J., and Naya J. E., *ApJ*, **526**, 200 (1999).
47. Timmes F.X., Woosley, S.E., Hartmann, D.H., *et al.*, *ApJ*, **464**, 332 (1996).
48. Tueller J., Barthelmy S., Gehrels N., *et al.*, *ApJ*, **351**, L41 (1990).
49. Vedrenne G., Roques J.-P., Schönfelder V., *et al.*, *A&A*, **411**, L63 (2003).
50. von Kienlin A., Attie D., Schanne S., *et al.*, *ESA-SP*, **552**, *in press* (2004).
51. Weidenspointner G., Lonjou V., Knödlseeder J., *et al.*, *ESA-SP*, **552**, *in press* (2004).
52. Winkler C., Courvoisier T. J.-L., Di Cocco G. *et al.* *A&A*, **411**, L1 (2003).
53. Zhu T., and Ruderman M, *ApJ*, **48**, 701 (1987).

